Gowrishankar et al., https://doi.org/10.1083/jcb.201612148

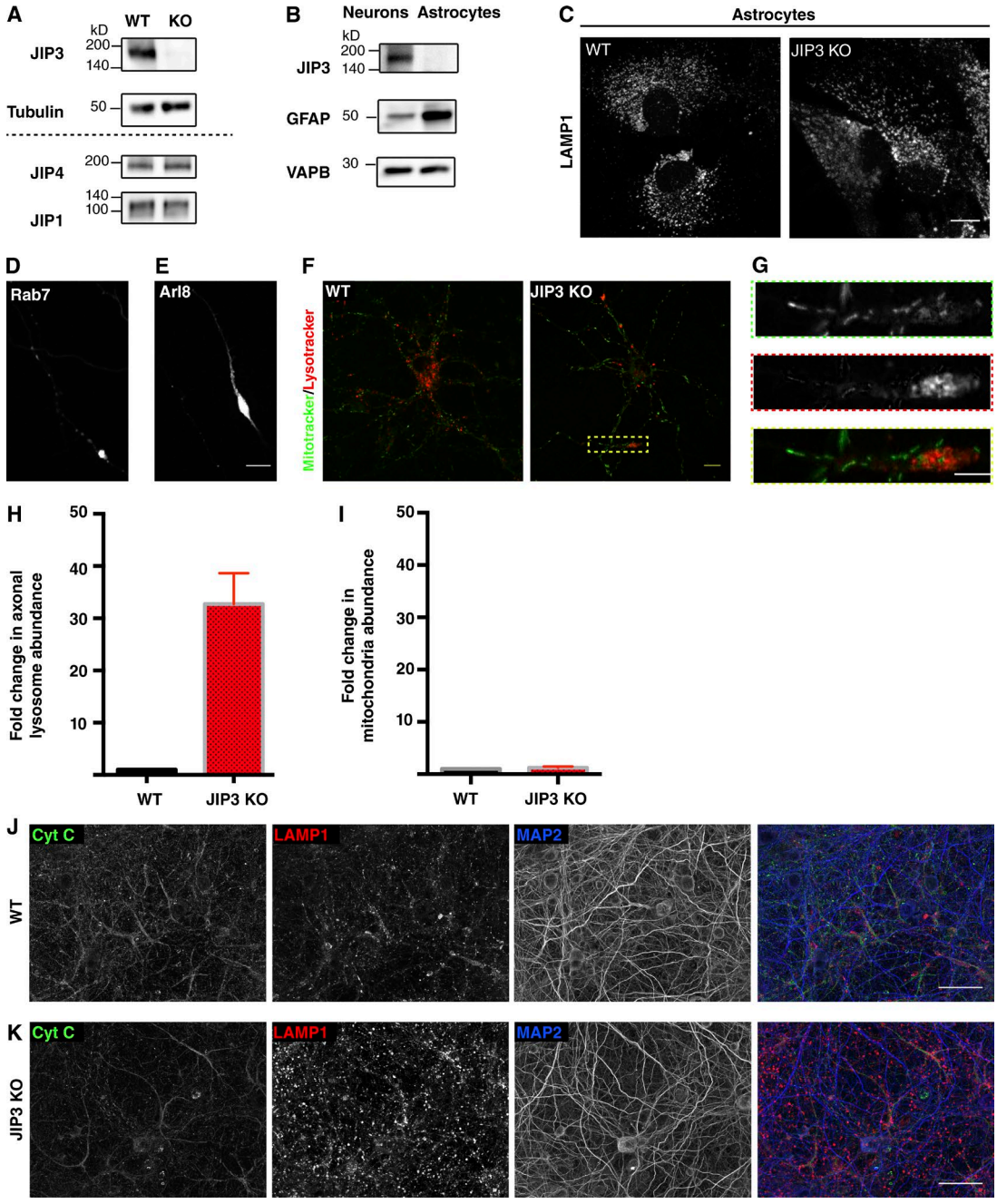

Figure S1. **Loss of JIP3 does not alter lysosome appearance in astrocytes or affect mitochondrial distribution in neurons.** (A) Western blot showing absence of JIP3 protein in lysates from JIP3 KO cultured neurons (14 DIV). Tubulin blot included as loading control. JIP4 and JIP1 levels in JIP3 KO neurons were not significantly changed compared with WT neurons (n = 3 independent experiments). (B) Immunoblotting of lysates from neuronal and astrocyte primary cultures shows that JIP3 levels are much higher in neurons than in astrocytes. (C) LAMP1 staining in WT and JIP3 KO astrocytes shows no change in lysosome distribution and morphology in WT versus JIP3 KO cells. (D and E) Images from JIP3 KO neurons (10 DIV) expressing GFP-Rab7 (D) or Arl8-GFP (E) showing enrichment of these proteins within axonal swellings. (F) LysoTracker (red) and MitoTracker (green) staining in WT and JIP3 KO neurons (10 DIV) grown at low density shows that although lysosomes accumulate massively in axonal swellings in JIP3 KO axons, mitochondria do not coaccumulate with them. Bar, 10 µm. (G) High-magnification image of a region of a JIP3 KO axon showing the accumulation of lysosomes and relative lack of enrichment of mitochondria in the swellings. Bar, 5 µm. (H and I) Quantification of the fold change in lysosome (H) and mitochondria (I) abundance in JIP3 KO axonal swellings compared with WT axons at similar distances from the cell body. Mean intensity measurements were made from four independent cultures (mean ± SD) from at least three to four neurons per experiment. (J and K) Stitched image of WT and JIP3 KO neurons (10 DIV) cultured at high density stained for cytochrome c (mitochondria), LAMP1 (lysosomes), and MAP2 (dendrites). Bars, 50 µm.

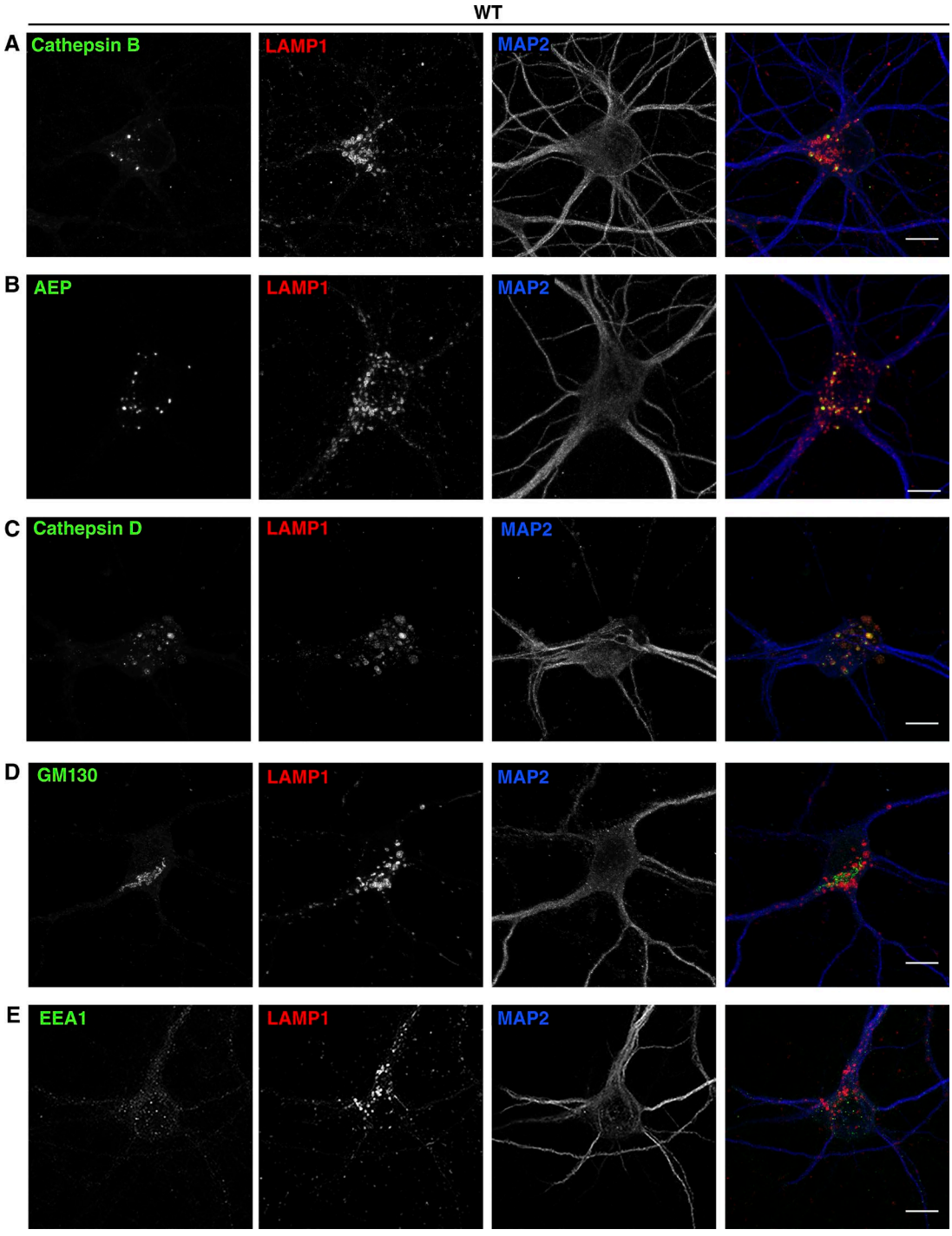

Figure S2. **Distribution of organelles and lysosomal enzymes in WT neurons.** (A–C) WT primary neurons (10–12 DIV) stained for lysosomal enzymes, cathepsin B (A), AEP (B), or cathepsin D (C) along with LAMP1 and MAP2. Although lysosomes in neuronal cell bodies are enriched in the soluble lysosomal proteases, the LAMP1 puncta in the neuritic processes have minimal levels of these proteins (A–C). (D and E) WT primary neurons (DIV 10–12) stained for Golgi (GM130) or early endosomes (EEA1), respectively, along with LAMP1 and MAP2. Bars, 10 µm.

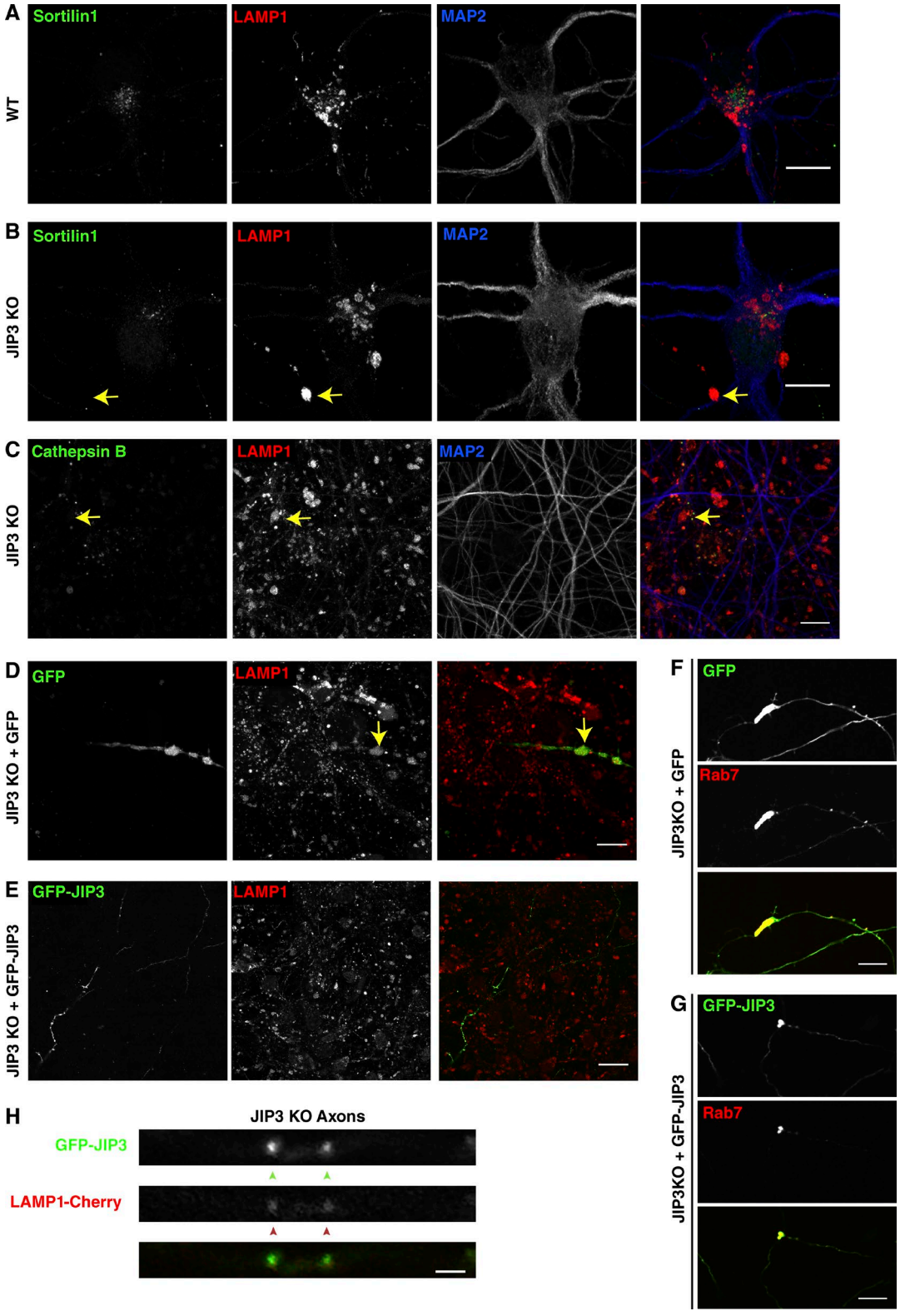

Figure S3. **Organelle composition of axonal swellings in JIP3 KO neurons and rescue after GFP-JIP3 expression.** (A and B) WT and JIP3 KO neurons (10 DIV) stained for sortilin 1, LAMP1 (lysosomes), and MAP2 show that there is no specific enrichment of sortilin 1–positive endosomal vesicles in the JIP3 KO axonal swellings (which are filled with lysosomes; arrows). Bars, 10 µm. (C) High-density culture of 10 DIV JIP3 KO neurons stained for cathepsin B (green), LAMP1 (red), and MAP2 (blue) highlights the relative lack of cathepsins in the axonal lysosome accumulations (arrows). Bar, 10 µm. (D and E) Anti-GFP and LAMP1 staining on fixed JIP3 KO neurons that were previously transfected with GFP (D) or GFP-JIP3 (E) showing that GFP-JIP3–expressing axons lack lysosome-filled axonal swellings, whereas surrounding untransfected neurons still have these lysosome accumulations. (F and G) JIP3 KO neurons transfected with Cherry-Rab7 and GFP (F) or Cherry-Rab7 and GFP-JIP3 (G) with lysosome-filled axonal swellings, depicting that even in the small fraction of GFP-JIP3–expressing KO neurons that still have the swelling, the lysosome accumulation is smaller, suggesting a partial rescue. Bars, 10 µm. (H) Portion of JIP3 KO axon transfected with GFP-JIP3 and Cherry-LAMP1 showing enrichment of GFP-JIP3 (green arrowheads) on lysosomes (red arrowheads). Bar, 2 µm.

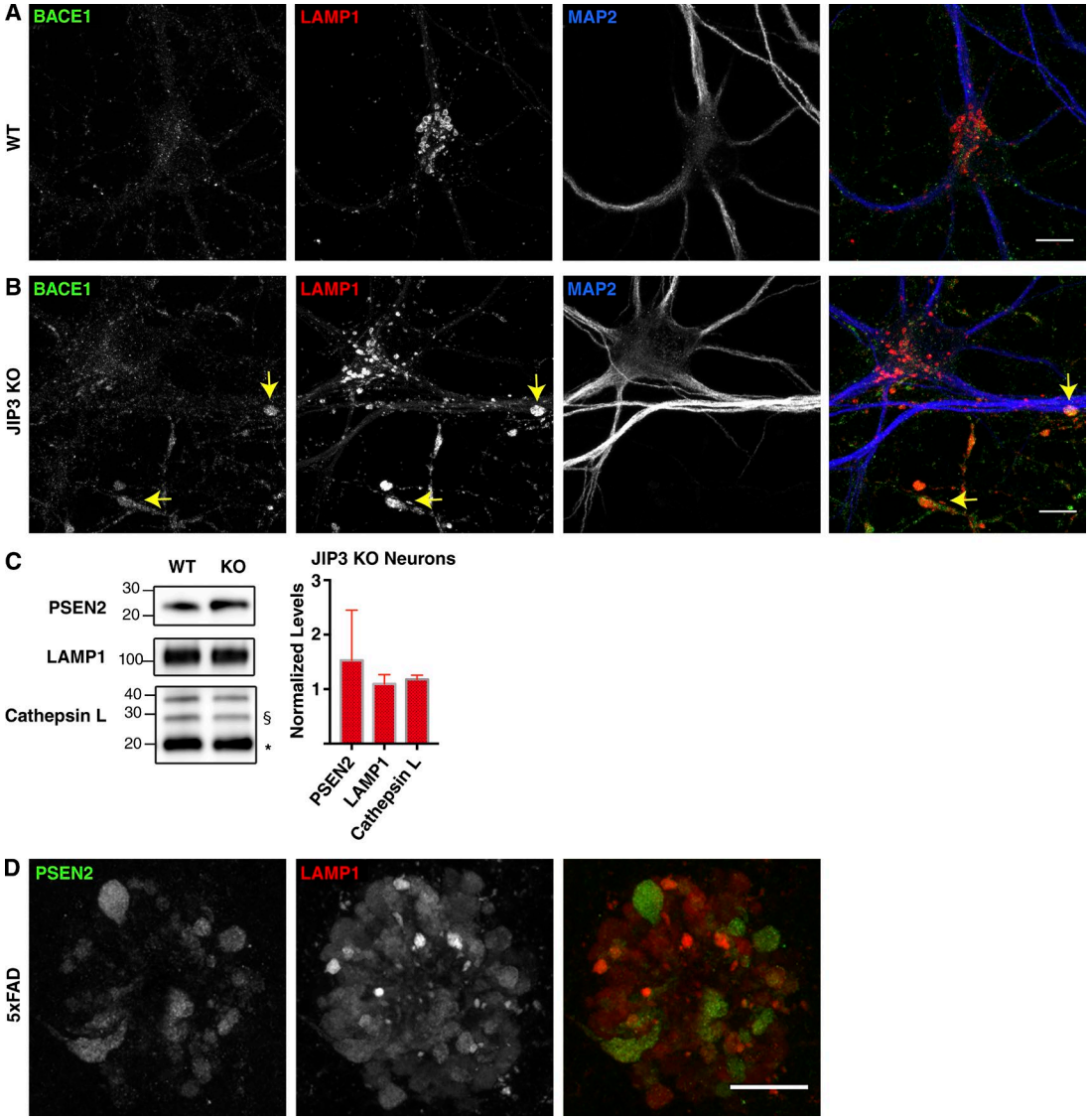

Figure S4. **Distribution and levels of APP-processing machinery in JIP3 KO neurons.** (A and B) Representative images of WT and JIP3 KO primary cortical neurons grown at low density and stained for BACE1 and LAMP1 (arrows highlight sites of axonal lysosome accumulation). Bars, 10 µm. (C) Western blot showing PSEN2, LAMP1, and cathepsin L levels in WT and JIP3 KO neurons (DIV 14) and quantification of levels of PSEN2, LAMP1, and cathepsin L (*, mature form; §, precursor form). Data are normalized to levels in WT (n = 3 independent cultures; mean ± SD). (D) PSEN2 (green) and LAMP1 (red) immunofluorescence staining in 5xFAD mouse brains showing their coaccumulation in plaque-associated dystrophic axons. Bar, 10 µm.

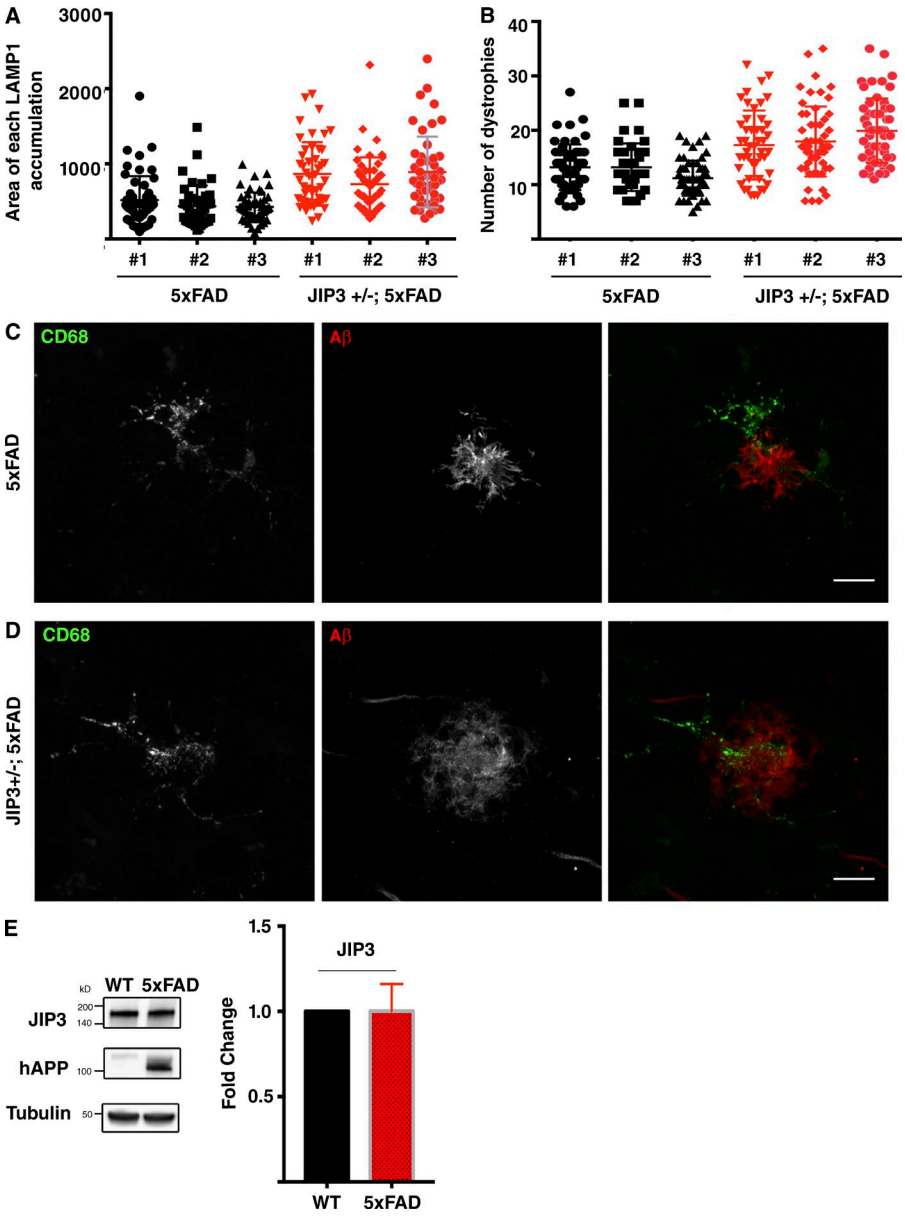

Figure S5. **Characterization of amyloid plaque pathology in JIP3 haploinsufficient mice.** (A) Distribution of area of LAMP1 accumulations around individual plaques from three pairs of female 5xFAD and JIP3+/−; 5xFAD littermates showing the increase in the mean area of lysosome accumulations in the JIP3 mutants (>45 plaques per animal per genotype were measured). (B) Distribution of the number of axonal swellings associated per amyloid plaque from three pairs of female 5xFAD and JIP3+/−; 5xFAD littermates showing the increase in the number of dystrophies per amyloid plaque in the JIP3 heterozygous mice. Swellings associated with at least 50 amyloid plaques per animal per genotype were counted. (C and D) Representative images from 5xFAD and JIP3+/−; 5xFAD littermates stained for CD68 (microglial lysosomes) and Aβ (plaque) showing that there is no obvious defect in microglial lysosomes in JIP3 haploinsufficient 5xFAD mice. Bars, 10 µm. (E) Western blot and quantification of JIP3 levels (mean ± SD) in the brains of WT and 5xFAD littermates show that levels of JIP3 are not altered in the 5xFAD mice.

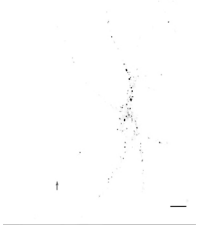

Video 1. **Video of LysoTracker dynamics in WT neurons shows there are very few LysoTracker-positive vesicles in the axon (gray arrow), which move predominantly in the retrograde direction.** In contrast, most of the lysosomes are found in the somatodendritic region and exhibit bidirectional transport. Images were acquired at 25 frames/min, playback rate is 7 frames/s. Bar, 10 µm.

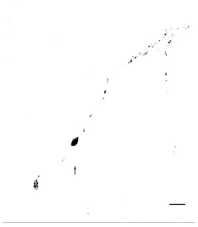

Video 2. **Video of LysoTracker dynamics in JIP3 KO neurons shows axonal swellings (gray arrow) filled with LysoTracker-positive structures.** Images were acquired at 25 frames/min, playback rate is 7 frames/s. Bar, 10 µm.

Table S1. **Antibody summary**

Antibody	Source	Catalog/clone number	Dilution
AEP/legumain	R&D Systems	AF2058	1:200 (IF)
Amyloid β	Cell Signaling Technology	2454	1:250 (IF)
APP	Millipore	22C11	1:1,000 (WB)
BACE-1	Cell Signaling Technology	5606	1:100 (IF); 1:1,000 (WB)
Cathepsin B	R&D Systems	AF965	1:200 (IF)
Cathepsin D	R&D Systems	AF1029	1:200 (IF)
Cathepsin L	R&D Systems	AF1515	1:1,000 (WB)
Cytochrome *c*	BD Biosciences	556432	1:100 (IF)
CD-68	ABD Serotech	MCA 1957T	1:250 (IF)
EEA1	Thermo Fisher Scientific	PAI-063A	1:100 (IF)
GFAP	Dako	Z0334	1:1,000 (WB)
GM130	BD Biosciences	610822	1:200 (IF)
Iba-1	Wako	019-19741	1:250 (IF)
JIP1	Santa Cruz Biotechnology	Sc-25267	1:1,000 (WB)
JIP3	Novous Biologicals	NBP1-00895	1:1,500 (WB)
JIP4	Cell Signaling Technology	5519	1:1,000 (WB)
LAMP1	Developmental Studies Hybridoma Bank	1D4B	1:250 (IF); 1:1,000 (WB)
MAP2b	BD Biosciences	610410	1:100 (IF)
MAP2b	Millipore	AB5622	1:500 (IF)
Neurofilament	Biolegend	SM312-R	1:200 (IF)
PSEN2	Abcam	Ab51249	1:100 (IF); 1:1,000 (WB)
Sortilin 1	Abcam	Ab16640	1:100 (IF)
Tubulin	Sigma Aldrich	T5168	1:10,000 (WB)
VAMP2	Synaptic Systems	C1 69.1	1:200 (IF)
VAPB	Sigma Aldrich	HPA013144	1:1,000 (WB)

IF, immunofluorescence experiments; WB, Western blotting experiments.

Table S2. **Plasmids used in the study**

Construct	Reference
GFP-Rab7	From Addgene (Choudhury et al., 2002)
Arl8-GFP	Provided by Thomas Melia (Yale University, New Haven, CT)
Cherry-Rab7	From Addgene (Rowland et al., 2014)
APP: VN+ BACE-1: VC	Provided by S. Roy (University of Wisconsin, Madison, WI; Das et al., 2016)
GFP-JIP3	This study

References

Choudhury, A., M. Dominguez, V. Puri, D.K. Sharma, K. Narita, C.L. Wheatley, D.L. Marks, and R.E. Pagano. 2002. Rab proteins mediate Golgi transport of caveola-internalized glycosphingolipids and correct lipid trafficking in Niemann-Pick C cells. *J. Clin. Invest.* 109:1541–1550. http://dx.doi.org/10.1172/JCI0215420

Das, U., L. Wang, A. Ganguly, J.M. Saikia, S.L. Wagner, E.H. Koo, and S. Roy. 2016. Visualizing APP and BACE-1 approximation in neurons yields insight into the amyloidogenic pathway. *Nat. Neurosci.* 19:55–64. http://dx.doi.org/10.1038/nn.4188

Rowland, A.A., P.J. Chitwood, M.J. Phillips, and G.K. Voeltz. 2014. ER contact sites define the position and timing of endosome fission. *Cell.* 159:1027–1041. http://dx.doi.org/10.1016/j.cell.2014.10.023